

Received: 2019.02.21

Accepted: 2019.03.21

Published: 2019.07.17

Mechanism of Cxc Chemokine Ligand 5 (CXCL5)/ Cxc Chemokine Receptor 2 (CXCR2) Bio-Axis in Mice with Acute Respiratory Distress Syndrome

Authors' Contribution:
Study Design A
Data Collection B
Statistical Analysis C
Data Interpretation D
Manuscript Preparation E
Literature Search F
Funds Collection G

ACDEF 1 **Chang-yong Wang**
BCF 1 **Min Shang**
BCF 2 **Chen-liang Zhou**
BCD 2 **Li-zhi Feng**
BDF 2 **Qing-shan Zhou**
A 1 **Ke Hu**

1 Division of Respiratory Disease, Renmin Hospital of Wuhan University, Wuhan, Hubei, P.R. China
2 Department of Critical Care Medicine, Renmin Hospital of Wuhan University, Wuhan, Hubei, P.R. China

Corresponding Author: Ke Hu, e-mail: huke_rmhospital@163.com
Source of support: Departmental sources

Background: Acute respiratory distress syndrome (ARDS) is a common acute and severe disease in clinic. Recent studies indicated that Cxc chemokine ligand 5 (CXCL5), an inflammatory chemokine, was associated with tumorigenesis. The present study investigated the role of the CXCL5/Cxc chemokine receptor 2 (CXCR2) bio-axis in ARDS, and explored the underlying molecular mechanism.

Material/Methods: The pathological morphology of lung tissue and degree of pulmonary edema were assessed by hematoxylin-eosin staining and pulmonary edema score, respectively. Real-time PCR and Western blot analysis were performed to detect the expression levels of CXCL5, CXCR2, Matrix metalloproteinases 2 (MMP2), and Matrix metalloproteinases 9 (MMP9) in lung tissues. Enzyme-linked immunosorbent assay (ELISA) was performed to determine the expression levels of CXCL5 and inflammatory factors (IL-1 β , IL-6, TNF- α , and IL-10) in serum.





Results: The results demonstrated that diffuse alveolar damage and pulmonary edema appeared in lipopolysaccharide (LPS)-induced ARDS and were positively correlated with the severity of ARDS. In addition, CXCL5 and its receptor CXCR2 were overexpressed by upregulation of MMP2 and MMP9 in lung tissues of ARDS. In addition, CXCL5 neutralizing antibody effectively alleviated inflammatory response, diffuse alveolar damage, and pulmonary edema, and decreased the expression levels of MMP2 and MMP9 compared to LPS-induced ARDS.

Conclusions: We found that CXCL5/CXCR2 accelerated the progression of ARDS, partly by upregulation of MMP2 and MMP9 in lung tissues with the release of inflammatory factors.

MeSH Keywords: **Chemokine CXCL5 • Inflammation • Respiratory Distress Syndrome, Adult**

Abbreviations: **ARDS** – acute respiratory distress syndrome; **CXCL5** – Cxc chemokine ligand 5; **CXCR2** – Cxc chemokine receptor 2; **MMP2** – matrix metalloproteinases 2; **MMP9** – matrix metalloproteinases 9; **LPS** – lipopolysaccharide; **UCC** – uterine cervix cancer; **H&E staining** – hematoxylin-eosin staining; **W/D** – wet-to-dry; **ELISA assay** – enzyme-linked immunosorbent assay; **SDS-PAGE** – sulfate polyacrylamide gel electrophoresis; **PVDF** – polyvinylidene fluoride; **TBST** – tris-buffered saline plus 0.1% Tween 20

Full-text PDF: <https://www.medscimonit.com/abstract/index/idArt/915835>

 2618   4  28



Background

Acute respiratory distress syndrome (ARDS) is a disease characterized by progressive dyspnea with refractory hypoxemia, which results from abnormal synthesis of pulmonary surfactant [1]. Obstinate hypoxemia and pulmonary edema in ARDS are caused by injury, shock, and other factors [2]. The pathological process of ARDS can be divided into 3 stages: the exudative stage (early stage), the proliferative stage (middle stage), and the fibrosis stage (late stage). At the exudative stage of ARDS, many cytokines and chemokines promote the pathological and physiological process of ARDS [3–5], showing that inflammation is closely related to the development of ARDS.

Chemokines, a group of the cytokines superfamily, have been divided into 4 conserved subfamilies (CXC, CX3C, CC, and C) based on the structural cysteine motifs adjacent to the NH2 terminus [6]. There is growing evidence that chemokines play an important role in tumorigenesis [7–9]. Cxc Chemokine Ligand 5 (CXCL5) presents a surprisingly elevated profile in bladder cancer cells, tissue, and urine of bladder cancer patients, and CXCL5 overexpression is critical for bladder cancer growth and progression [10]. CXCL5, by binding to its cell-surface receptor Cxc Chemokine Receptor 2 (CXCR2), plays an oncogenic role in many human cancers. The serum protein expression of CXCL5 is significantly increased in non-small cell lung cancer (NSCLC) compared with that in healthy volunteers [11]. The expression of CXCL5 was significantly higher in lung cancer cell lines, and high CXCL5 was associated with high CXCR2 expression, which was significantly associated with poor differentiation [12]. CXCL5/CXCR2 performs its roles in angiogenesis, immune response, and tumor progression [13,14]. CXCL5 is an inflammatory chemokine, which is a member of the same family as CXCL10 [15]. CXCL10 can promote the development of inflammation in ARDS [16]. However, the role of CXCL5 in ARDS and its associated mechanisms are still unknown, as is whether it participates in the inflammatory process of ARDS by binding to its receptor CXCR2.

In the present study we investigated the role of the CXCL5/CXCR2 bio-axis in ARDS and the underlying molecular mechanism involved to provide a theoretical basis for clinical targeted gene therapy.

Material and Methods

Animals

Male C57BL/6 mice (male, 5–6 weeks, weighing 18–20 g) were purchased from Chongqing TengXin Biological Technology Co. Prior to the experiments, 50 mice were maintained in an environmentally controlled room (22°C±2°C, 12 h light-12 h dark

cycle) with free access to food and water for 7 days to acclimatize to the new environment. The animal protocol was approved by the Laboratory Animal Care and Use Committee at Renmin Hospital of Wuhan University (IACUC Issue No. 20180506; Date: 20180507).

Mouse model of acute respiratory distress syndrome (ARDS)

Fifty male mice were randomly divided into a normal saline control group (n=5) and an LPS-induced group composed of 3 groups: the LPS-4h group, the LPS-8h group, and the LPS-12h group, with 15 mice in each group. All mice were given abdominal anaesthesia with sodium barbiturate. Mice in the LPS-induced group were subjected to endotracheal instillation of 200 µg/kg LPS for 4 h, 8 h, and 12 h, respectively. Mice in the normal saline control group were subjected to endotracheal instillation of 200 µg/kg saline. After the best time point of LPS-induced ARDS was obtained, another 10 mice in the best time point of the LPS-induced group were randomly divided into an LPS+anti-CXCL5 group (n=5) and an LPS+IgG group (n=5). The mice in the LPS+anti-CXCL5 group and LPS+IgG group were intraperitoneally injected with 50 µg CXCL5 neutralizing antibody or 50 µg IgG control, respectively, at 1 h after LPS induction.

Hematoxylin-eosin staining (HE staining)

The lung tissue was fixed in 4% paraformaldehyde for 12 h, then embedded in paraffin. The paraffin-embedded lung tissue was sliced into 5-µm-thick sections. The sections were dewaxed for 30 min each time (xylene, repeated 3 times), rehydrated for 5 min in gradient ethanol (non-water ethanol, 95% ethanol, 80% ethanol, 70% ethanol, and 50% ethanol), washed with distilled water for 5 min, and stained with hematoxylin for 5 min. Then, distilled water was used to wash off the excess hematoxylin, followed by dehydration using gradient ethanol (50% ethanol, 70% ethanol, and 80% ethanol) and stained with eosin for 1 min. Finally, the slices were dehydrated using alcohol and transparentized with xylene for 5 min, which sealed with neutral balsam. The slides were observed under an inverted fluorescence microscope (MF53; Micro-shot Technology Co., Guangzhou, China).

Pulmonary edema score

After the foreign matter on the surface of the right lung middle lobe was cleared, the wet weight of the right lung middle lobe was immediately weighed. Then, the lung tissue was dried in an oven at 80°C for 72 h and the dry weight was immediately assessed. The wet-to-dry (W/D) ratio of lung tissue was calculated for pulmonary edema score according to the lung injury score. The degree of pulmonary edema was determined by the pulmonary edema score according to wet/dry ratio.

Enzyme-linked immunosorbent assay (ELISA assay)

Blood (0.5 mL) was taken from mice of each group through eyeball extraction, and serum was separated by centrifugation at 4000 rpm for 10 min at 4°C and stored at -80°C. An ELISA kit Shanghai Jianglai Biotechnology Co., Shanghai, China) was used to measure CXCL5 expression and IL-1 β , IL-6, TNF- α , and IL-10 expressions (Shanghai Enzyme-Linked Biotech Co., Shanghai, China) following the manufacturer's protocol. The 96-well microplates were read using a microplate reader (Thermo, Waltham, MA) at 450 nm.

Western blotting

Briefly, lung tissues were put on ice and cut into pieces using sterile scissors. We homogenized 50 mg lung tissue using 500 μ L RIPA lysis buffer (Beyotime, Shanghai, China) placed on ice to lyse for 30 min. Then, total protein of lung tissues was collected after centrifugation (12 000 rpm, 4°C) which was assessed using a BCA Protein Assay Kit (Pierce; Thermo Fisher Scientific) to determine the concentration. Equal quantities (30 μ g) of proteins per lane were subjected to 12% sodium dodecyl sulfate polyacrylamide gel electrophoresis (SDS-PAGE) gels and transferred to polyvinylidene fluoride (PVDF) membranes (Merck Millipore, Billerica, MA). After transfer, 5% nonfat milk in TBST (Tris-buffered saline plus 0.1% Tween 20) was applied to block the nonspecific binding sites on the membranes for 1 h. Then, the membranes were incubated overnight at 4°C with primary antibody against CXCL5 (ab9983; Cell Signaling Technology, USA; dilution, 1: 1000), CXCR2 (ab14935; Cell Signaling Technology, USA; dilution, 1: 500), MMP2 (ab92536; Cell Signaling Technology, USA; dilution, 1: 1000), and MMP9 (ab38898; Cell Signaling Technology, USA; dilution, 1: 1000). Subsequently, horseradish peroxidase-conjugated goat anti-rabbit secondary antibody (Beyotime) was added and membranes were incubated at room temperature for 2–3 h. Finally, the results of protein bands were visualized with an enhanced chemiluminescence detection system (Super Signal West Dura Extended Duration Substrate; Thermo Fisher Scientific).

Real-time PCR

Briefly, lung tissues were quickly ground in a mortar with a small amount of liquid nitrogen. The above process was repeated 3 times. We homogenized 50 mg lung tissue using 1 mL Trizol with an electric homogenizer for 1–2 min. After centrifugation at 12 000 rpm for 5 min, the supernatant was discarded and 200 μ L chloroform was added into the centrifuge tube, which was vibrated for 15 s and then allowed to stand for about 10 min at room temperature. Then, after centrifugation at 12 000 rpm for 15 min at 4°C, the upper water phase in the centrifuge tube was transferred to a new centrifuge tube and mixed well with 0.6 ml isoamylol and allowed to stand for 5–10 min at room

temperature. After centrifugation at 12 000 rpm for 15 min at 4°C, the supernatant was discarded and 1 mL of 75% ethanol was added into the centrifuge tube, which was vibrated gently, and the total RNA precipitate was suspended and then dried at room temperature. Total RNA was isolated from the lung tissue using a total RNA extraction kit (Beijing Tianenze Gene Technology Co., Beijing, China) and we produced cDNA using a RT-qPCR kit (Hangzhou Bioer Technology Co., Zhejiang, China). The thermocycling conditions were as follows: Initial denaturation at 95°C for 2 min; denaturation at 95°C for 30 s; annealing at 59°C for 45 s; elongation at 72°C for 60 s for 30 cycles; and elongation at 72°C for 7 min. GAPDH was used as the endogenous control for the expression levels of mRNA. The primer sequences for qPCR were as follows: GAPDH forward, 5'-TATGTCGTGGAGTCTACTGG-3', and reverse, 5'-AGTGATGGCATGGACTGTGG-3'; CXCL5 forward, 5'-CTCAGTCATAGCCGCAACCGAGC-3', and reverse, 5'-CGCTTCTTTCCACTGCGAGTGC-3'; CXCR2 forward, 5'-TCTGCTCACAACAGCGTCGTA-3', and reverse, 5'-GAGTGGCATGGGACAGCATC-3'; MMP2 forward, 5'-GACGCTGCCTTTAACTGGAGT-3', and reverse, 5'-TCCAGTTATCAGGGATGGCA-3'; MMP9 forward, 5'-CCTGGAACCTACACAAGTCT-3', and reverse, 5'-GCAGGAGGCATAGTACAG-3'. The relative quantification of gene expression was measured by the method of 2^{- $\Delta\Delta$ Cq}.

Statistical analysis

All experimental values are expressed as the mean \pm standard deviation. Statistical analyses were performed using GraphPad Prism 5 software. The *t* test was used to analyze difference between 2 groups and differences between the multiple groups were analyzed by one-way ANOVA. *P*<0.05 was considered statistically significant.

Results

LPS induced physiological response, lung pathological manifestations, and pulmonary edema in mice

Mice in the normal saline control group showed no abnormal manifestations. In the LPS induced group, mice showed significantly increased respiratory rate and heart rate, obvious cyanosis of the lips and limbs, slow reaction, and decreased activity with prolonged administration time.

To observe the pathological changes of the lung tissues, hematoxylin and eosin (HE) staining and pulmonary edema score were used. As shown in Figure 1A, there was no obvious pathological lung changes in the normal saline control group. Significantly pathological manifestations in the lung were observed in the

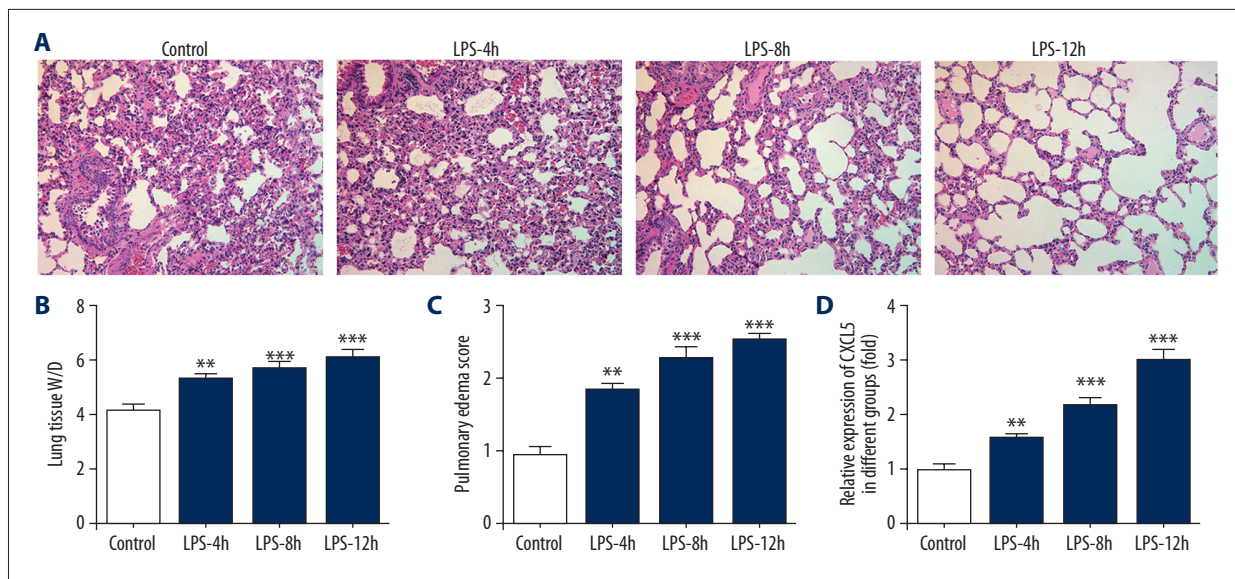


Figure 1. The changes in mice resulting from LPS treatment. (A) Lung pathological changes. (B) Wet-to-dry (W/D) ratio of lung tissue. (C) Lung pathological changes. (D) Level of CXCL5 in the blood. ** P<0.01 and *** P<0.001 vs. control group. LPS-4h group, group treated with LPS for 4 h. LPS-8h group, group treated with LPS for 8 h. LPS-12h group, group treated with LPS for 12 h.

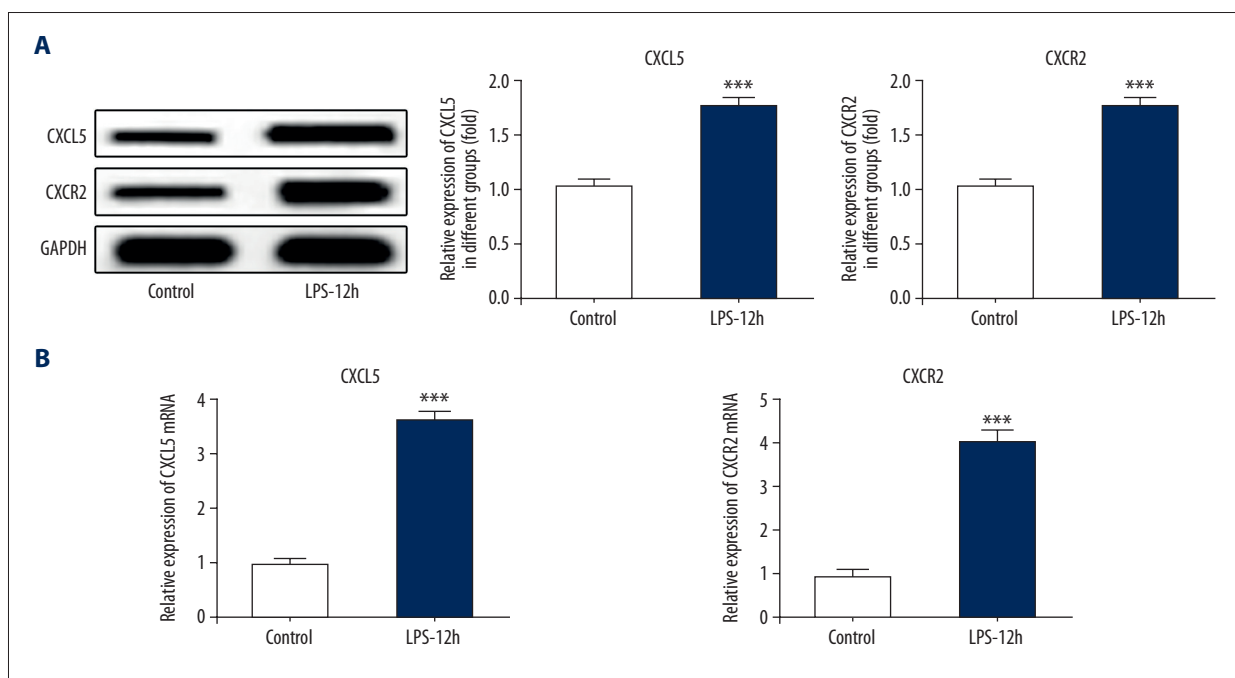


Figure 2. The expression of CXCL5 and CXCR2 in lung tissues determined by Western blot and RT-qPCR. (A) Results of Western blot for CXCL5 and CXCR2. (B) Results of RT-qPCR for CXCL5 and CXCR2. *** P<0.001 vs. control group. LPS-12h group, group treated with LPS for 12 h.

LPS-induced groups, including alveolar congestion, hemorrhage, edema, infiltration of inflammatory cell in the airspace, atelectasis, and hyaline membrane formation. As shown in Figure 1B and 1C, the lung tissue W/D and pulmonary edema scores were both obviously increased by LPS intervention and gradually increased with prolonged administration time.

Expression of CXCL5 and CXCR2 in lung tissues of acute respiratory distress mice induced by LPS

Blood was collected before the mice were killed, and the expression of CXCL5 in the blood was analyzed by ELISA. As shown in Figure 1D, the expression of CXCL5 in the LPS-induced group

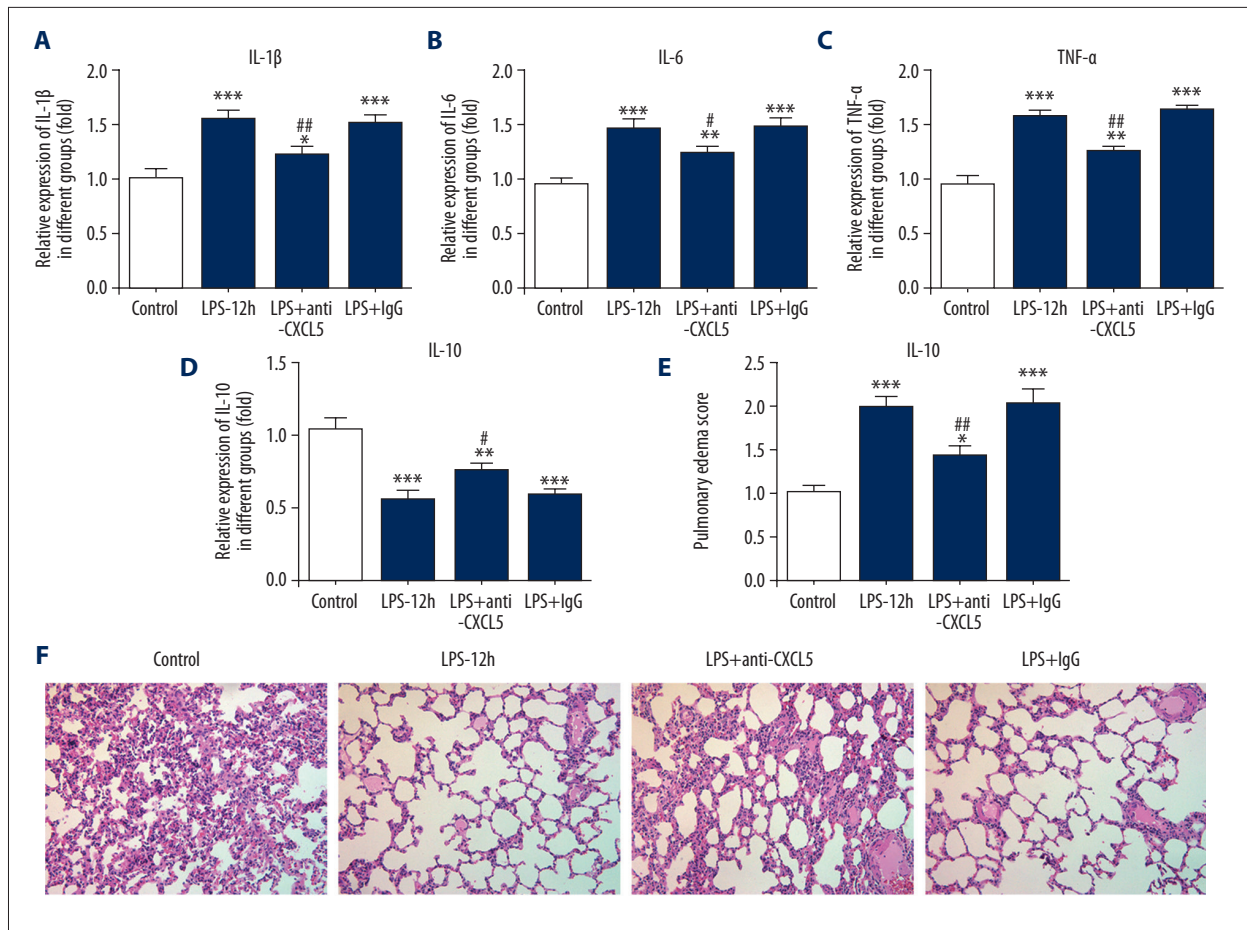


Figure 3. Neutralization of CXCL5 can alleviate LPS induced ARDS. (A) Level of IL-1 β in the blood. (B) Level of IL-6 in the blood. (C) Level of TNF- α in the blood. (D) Level of IL-10 in the blood. (E) Pulmonary edema score. (F) Lung pathological changes. * $P < 0.05$ and ** $P < 0.01$ and *** $P < 0.001$ vs. control group. # $P < 0.05$ and ## $P < 0.01$ vs. LPS-12h group. LPS-12h group, group treated with LPS for 12 h. LPS+anti-CXCL5 group, group treated with LPS and CXCL5. LPS+IgG group, group treated with LPS and CXCL5.

was higher than in the normal saline control group and increased with the extension of the induction time (4, 8, and 12 h). Therefore, 12 h was selected as the induction time for the following experiments.

To determine the expression of CXCL5 and CXCR2 in lung tissues, Western blot and RT-qPCR analyses were performed. As shown in Figure 2A and 2B, the expression of CXCL5 and CXCR2 and CXCL5 and CXCR2 mRNAs in lung tissues were all increased in the LPS-12h group compared with the normal saline control group. The above results suggest that the role of CXCL5 in ARDS may be mediated by CXCR2.

Neutralization of CXCL5 can alleviate LPS-induced ARDS

The changes of inflammatory factors (IL-1 β , IL-6, TNF- α , and IL-10) in the blood were determined by ELISA assay in the normal saline control group, the LPS-12h group, the LPS+CXCL5 group, and the LPS+IgG group. As shown in Figure 3A–3D,

compared with the LPS-12h group, the expressions of IL-1 β , IL-6, and TNF- α were decreased in the LPS+CXCL5 group but were higher than in the normal saline control group, and the expression of IL-10 was higher than in the LPS+CXCL5 group but lower than in the normal saline control group.

The changes of pulmonary edema were observed by calculating the wet-to-dry (W/D) ratio of lung tissue. As shown in Figure 3E, compared with the LPS-12h group, pulmonary edema in the LPS+CXCL5 group was alleviated, but it was slightly more serious than in the normal saline control group. Pulmonary edema in the LPS+IgG group was similar to that in the LPS-12h group.

The lung pathological changes were detected by HE staining. As shown in Figure 3F, compared with LPS-12h group, lung pathological change in the LPS+CXCL5 group was attenuated, but it was slightly greater than in the normal saline control group. Additionally, no obvious difference in lung pathological

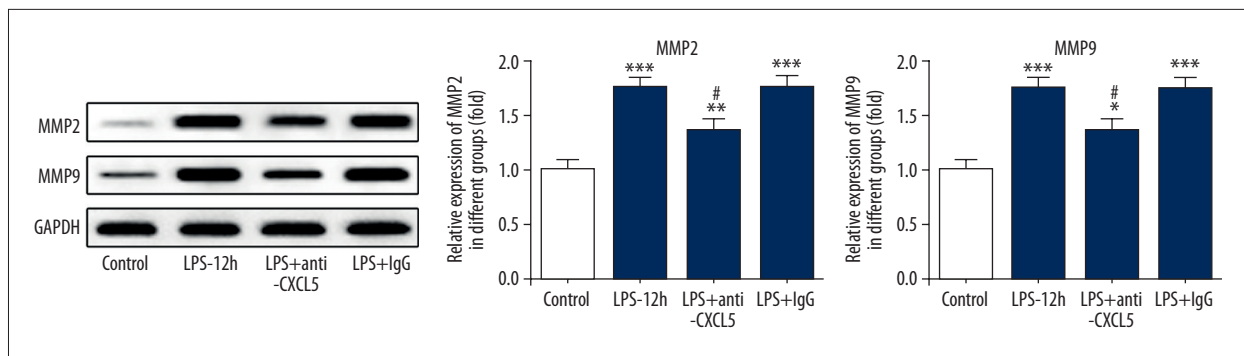


Figure 4. CXCL5 and CXCR2 aggravate ARDS progression by promoting the expression of MMP2 and MMP9. The expression of MMP2 and MMP9 in lung tissues as determined by Western blot and RT-qPCR. * $P < 0.05$ and ** $P < 0.01$ and *** $P < 0.001$ vs. control group. # $P < 0.05$ vs. LPS-12h group. LPS-12h group, group treated with LPS for 12 h. LPS+anti-CXCL5 group, group treated with LPS and CXCL5. LPS+IgG group, group treated with LPS and CXCL5.

change was found between the normal saline control group and the LPS+IgG group.

CXCL5 and CXCR2 aggravate ARDS progression by promoting the expression of matrix metalloproteinase-2 (MMP2) and matrix metalloproteinase-9 (MMP9)

The expressions of MMP2 and MMP9 in lung tissues were determined by Western blot and RT-qPCR analyses in the normal saline control group, the LPS-12h group, the LPS+CXCL5 group, and the LPS+IgG group. As shown in Figure 4, compared with normal saline control group, the expression of MMP2 and MMP9 in lung tissues was higher in the LPS-12h group, while it was lower than in the LPS+CXCL5 group. The expressions of MMP2 and MMP9 in lung tissues in the LPS+IgG group were similar to those in the LPS-12h group. These results indicated that MMP2 and MMP9 overexpression exacerbate ARDS progression.

Discussion

Here, we investigated the mechanism and function of the CXCL5/CXCR2 bio-axis in mice with ARDS, showing that overexpression of CXCL5 and CXCR2 can aggravate ARDS progression by promoting the expression of MMP2 and MMP9.

ARDS is a disease that can be caused by severe infection, trauma, shock, surgery, or aspiration. The main pathological feature of ARDS is that inflammation is resulted in increased pulmonary microvascular permeability and protein-rich fluid is exuded from the alveolar cavity, which leads to pulmonary edema and transparent membrane formation, accompanied by alveolar hemorrhage. Therefore, inflammation is an essential factor in the development of ARDS.

Chemokines are important for the construction of the tumor microenvironment. CXC-chemokines, as the second subgroup

of chemokines, seem to be present in almost all processes of tumor progression [17]. Many studies have demonstrated that CXCL5 participates in the development of lung cancer [18,19]. In addition to their function in tumor progression, the CXC-chemokines were reported to be related to the development of ARDS, including CXCL8 [20], CXCL10 [21], and CXCL1 [22]. CXCL5 and the previously studied CXC-chemokines (CXCL8, CXCL10, and CXCL1) all belong to the same family. A previous study showed that CXCL5 was involved in acute bacterial pneumonia [23]. We predicted that CXCL5 also functioned in ARDS. In the present study, we observed that the expression of CXCL5 was obviously increased in LPS-induced ARDS and gradually increased with disease progression. In addition, neutralization of CXCL5 can decrease the release of inflammatory factors, reduce pulmonary edema and pathological injury, thus alleviating LPS-induced ARDS.

CXCR2 is a typical G-protein-coupled receptor (GPCR), and can be bound and activated by CXCL5. CXCR2 is the main receptor for the regulation of inflammatory neutrophil recruitment in acute and chronic inflamed tissues [24]. CXCR2 was demonstrated to be related to the pathogenesis and progress of acute lung injury and ARDS [25]. Our results are consistent with a previous report [26] that the expression of CXCR2 is directly proportional to the severity of ARDS, and the role of CXCL5 in ARDS may be mediated by CXCR2.

The activation of MMP2 and MMP9 is involved in alveolar macrophages during acute lung injury, which can exacerbate pulmonary inflammation [27]. Matrix metalloproteinases (MMPs) are particularly potent in degrading basement membrane collagen, which is associated with lung injury in inflammatory processes [28]. We hypothesized that MMPs aggravated the progression of acute lung injury and we demonstrated that overexpression of MMP2 and MMP9 caused deterioration of LPS-induced ARDS.

Conclusions

We found that upregulation of CXCL5 promoted the progression of LPS-induced ARDS, which was mediated by correspondingly increased CXCR2. CXCL5/CXCR2 accelerated the progression of ARDS, partly by upregulation of MMP2 and MMP9 in lung tissues with the release of inflammatory factors. To the best of our knowledge, this is the first study to reveal the

mechanism of CXCL5/CXCR2 and to elucidate the function of MMP2 and MMP9 in ARDS, which could result in new therapeutic options against ARDS in the future.

Conflicts of Interest

The authors declare they have no competing interests.

References:

1. Quasney MW, Lopez-Fernandez YM, Santschi M et al: The outcomes of children with pediatric acute respiratory distress syndrome: Proceedings from the Pediatric Acute Lung Injury Consensus Conference. *Pediatr Crit Care Med*, 2015; 16(5 Suppl. 1): S118-31
2. Balk RA: Incidence and outcomes of acute lung injury. *Yearbook of Critical Care Medicine*, 2007; 2007(4): 29-30
3. Schwingshackl A, Teng B, Makena PS et al: Regulation and function of the two-pore-domain potassium (K2P) channel *Trek-1* in acute lung injury. *American Thoracic Society 2011 International Conference*, May 13-18, 2011, Denver Colorado, 2011; A4235.
4. Schwingshackl A, Teng B, Ghosh M et al: Regulation of interleukin-6 secretion by the two-pore-domain potassium channel *Trek-1* in alveolar epithelial cells. *Am J Physiol Lung Cell Mol Physiol*, 2013; 304(4): L276-86
5. Andreas S, Bin T, Manik G et al: Regulation of monocyte chemotactic protein-1 secretion by the two-pore-domain potassium (K2P) channel *TREK-1* in human alveolar epithelial cells. *Am J Transl Res*, 2013; 5(5): 530-42
6. Liu Q, Li A, Tian Y et al: The CXCL8-CXCR1/2 pathways in cancer. *Cytokine Growth Factor Rev*, 2016; 31: 61-71
7. Poeta VM, Massara M, Capucetti A et al: Chemokines and chemokine receptors: New targets for cancer immunotherapy. *Front Immunol*, 2019; 10: 379
8. Chen C, He W, Huang J et al: LNMAT1 promotes lymphatic metastasis of bladder cancer via CCL2 dependent macrophage recruitment. *Nat Commun*, 2018; 9(1): 3826
9. Sun ZR, Du CC, Xu PB et al: Surgical trauma-induced CCL18 promotes recruitment of regulatory T cells and colon cancer progression. *J Cell Physiol*, 2019; 234(4): 4608-16
10. Zhu X, Qiao Y, Liu W et al: CXCL5 is a potential diagnostic and prognostic marker for bladder cancer patients. *Tumor Biol* 2016; 37(4): 4569-77
11. Wu KJ, Yu SN, Liu Q et al: The clinical significance of CXCL5 in non-small cell lung cancer. *OncoTargets Ther*, 2017; 10: 5561-73
12. Wang L, Shi L, Gu J et al: CXCL5 regulation of proliferation and migration in human non-small cell lung cancer cells. *J Physiol Biochem*, 2018; 74(2): 313-24
13. Zhou SL, Zhou ZJ, Hu ZQ et al: CXCR2/CXCL5 axis contributes to epithelial-mesenchymal transition of HCC cells through activating PI3K/Akt/GSK-3 β /Snail signaling. *Cancer Lett*, 2015; 358(2): 124-35
14. Gao Y, Guan ZF, Chen JQ et al: CXCL5/CXCR2 axis promotes bladder cancer cell migration and invasion by activating PI3K/AKT-induced upregulation of MMP2/MMP9. *Int J Oncol*, 2015; 47(2): 690-700
15. He SQ: [Chemokines and immunomodulatory cytokines.] *Immunological Journal*, 2003 [in Chinese]
16. Lang S, Li LB, Wang XN et al: CXCL10/IP-10 neutralization can ameliorate lipopolysaccharide-induced acute respiratory distress syndrome in rats. *PLoS One*, 2017; 12(1): e169100
17. Lee HJ, Song IC, Yun HJ et al: CXC chemokines and chemokine receptors in gastric cancer: From basic findings towards therapeutic targeting. *World J Gastroenterol*, 2014; 20(7): 1681-93
18. Kuo PL, Huang MS, Hung JY et al: Synergistic effect of lung tumor-associated dendritic cell-derived HB-EGF and CXCL5 on cancer progression. *Int J Cancer*, 2014; 135(1): 96-108
19. Kowalczyk O, Burzykowski T, Niklinska WE et al: CXCL5 as a potential novel prognostic factor in early stage non-small cell lung cancer: Results of a study of expression levels of 23 genes. *Tumor Biol*, 2014; 35(5): 4619-28
20. Hashemian SMR, Mortaz E, Tabarsi P et al: Elevated CXCL-8 expression in bronchoalveolar lavage correlates with disease severity in patients with acute respiratory distress syndrome resulting from tuberculosis. *J Inflamm (Lond)*, 2014; 11: 21
21. Tang NLS, Chan PKS, Wong CK et al: Early enhanced expression of interferon-inducible protein-10 (CXCL-10) and other chemokines predicts adverse outcome in severe acute respiratory syndrome. *Clin Chem*, 2005; 51(12): 2333-40
22. Deroost K, Tyberghein A, Lays N et al: Hemozoin induces lung inflammation and correlates with malaria-associated acute respiratory distress syndrome. *Am J Respir Cell Mol Biol*, 2013; 48(5): 589-600
23. Traber KE, Hilliard KL, Allen E et al: Induction of STAT3-dependent CXCL5 expression and neutrophil recruitment by oncostatin-M during pneumonia. *Am J Respir Cell Mol Biol*, 2015; 53(4): 479-88
24. Cao Q, Li BR, Wang XK et al: Therapeutic inhibition of CXC chemokine receptor 2 by SB225002 attenuates LPS-induced acute lung injury in mice. *Arch Med Sci*, 2018; 14(3): 635-44
25. Aziz M, Matsuda A, Yang WL et al: Milk fat globule-epidermal growth factor-factor 8 attenuates neutrophil infiltration in acute lung injury via modulation of CXCR2. *J Immunol*, 2012; 189(1): 393-402
26. Li Y, Huang J, Foley NM et al: B7H3 ameliorates LPS-induced acute lung injury via attenuation of neutrophil migration and infiltration. *Sci Rep*, 2016; 6: 31284
27. Liang YF, Yang NL, Pan GQ et al: Elevated IL-33 promotes expression of MMP2 and MMP9 via activating STAT3 in alveolar macrophages during LPS-induced acute lung injury. *Cell Mol Biol Lett*, 2018; 23: 52
28. Corbel M, Lagente V, Theret N et al: Comparative effects of betamethasone, cyclosporin and nedocromil sodium in acute pulmonary inflammation and metalloproteinase activities in bronchoalveolar lavage fluid from mice exposed to lipopolysaccharide. *Pulm Pharmacol Ther*, 1999; 12(3): 165-71